

Measurement System of Small-Scale High Expansion Ratio ORC Turbine

Uusitalo Antti, Zocca Marta, Turunen-Saaresti Teemu

This is a Final draft version of a publication

published by Springer, Cham

in Pini, M., De Servi, C., Spinelli, A., di Mare, F., Guardone, A. (eds) Proceedings of the 3rd International Seminar on Non-Ideal Compressible Fluid Dynamics for Propulsion and Power. NICFD 2020. ERCOFTAC Series, vol 28.

DOI: 10.1007/978-3-030-69306-0_12

Copyright of the original publication:

© The Author(s), under exclusive license to Springer Nature Switzerland AG 2021

Please cite the publication as follows:

Uusitalo, A., Zocca, M., Turunen-Saaresti, T. (2021). Measurement System of Small-Scale High Expansion Ratio ORC Turbine. In: Pini, M., De Servi, C., Spinelli, A., di Mare, F., Guardone, A. (eds) Proceedings of the 3rd International Seminar on Non-Ideal Compressible Fluid Dynamics for Propulsion and Power. NICFD 2020. ERCOFTAC Series, vol 28. Springer, Cham. DOI: 10.1007/978-3-030-69306-0_12

**This is a parallel published version of an original publication.
This version can differ from the original published article.**



Measurement system of small-scale high expansion ratio ORC turbine

Antti Uusitalo
LUT University
antti.uusitalo@lut.fi
Lappeenranta, Finland

Marta Zocca
LUT University
marta.zocca@lut.fi
Lappeenranta, Finland

Teemu Turunen-Saaresti
LUT University
teemu.turunen-saaresti@lut.fi
Lappeenranta, Finland

ABSTRACT

Small-scale and high temperature ORCs have received increasing interest in recent times. This type of power systems can have high expansion ratio turbines with gas dynamic effects differing significantly from the behaviour of ideal gases, as the turbines are often operated in the non-ideal dense-gas region. One of the most crucial steps leading to future improvement of turbine efficiency and to the development of design guidelines and loss analysis methods is to validate the applied design methods and loss correlations with experimental data. However, accurately measuring the performance of ORC turbines can be challenging. Indeed, despite the high pressure ratios, the temperature drop across the turbines remains rather low, and the physical size of turbomachinery tends to be small. In this paper, updates to the measurement system of the 10 kW LUT micro-ORC test-rig operating with siloxane MDM are presented. Further measurement points are placed at turbine inlet and outlet, and inside the turbine stator, with the aim of obtaining accurate performance maps and turbine loss analysis from future experimental runs.

Keywords: ORC turbine, turbine measurements, dense gas flows

1 INTRODUCTION

Small-scale (about 10 kW to 50 kW) ORCs have been intensively studied in recent times. Especially in high-temperature small-scale ORCs, fluids with high molecular weight and with relatively high critical temperature are adopted. This type of fluids are characterized by gas dynamic effects that differ significantly from those of ideal gases, especially if the turbine of the system is designed to operate in the dense-gas region. The use of high molecular weight and critical temperature fluids in ORCs also often results in high expansion ratio over the turbine, whereas simultaneously the temperature drop remains moderate. In addition, as the speed of sound of these fluids is rather low, the turbine stator has to be designed for highly supersonic flow conditions [1]. There are not many experimental studies on small-scale high temperature ORC turbines in the present literature, see e.g. Ref. [7, 2]. Thus, it is crucial to carry out more experimental research on small ORC turbines. Due to the gas dynamic effects of organic fluids, it is still unclear how such turbines should be designed in respect to the more conventional turbomachinery design guidelines. In addition, it is still unclear what is the contribution of different individual loss sources on the overall losses of ORC turbines.

In this paper, the updated turbine measurement system of the LUT micro ORC test setup is presented. The system has a 10 kW scale highly supersonic radial turbine, and uses siloxane MDM as a working fluid. The turbine inlet pressure of 7.9 bar, temperature of 265 °C, fluid mass flow rate of 0.2 kg/s and turbine outlet pressure of about 0.07 bar were defined as the turbine design operating conditions. More details on the operating points of the setup and the working fluid selection are described in Ref. [4]. Several test were run with the facility, and the system turbogenerator was successfully operated with the design operating conditions with rotational speeds of up to 30 000 rpm, see e.g. Ref. [5]. However, in the experiments carried out so far, it was observed that accurately defining the turbine performance during the experiments is sensitive especially on the accuracy of turbine outlet state measurements, namely the turbine outlet temperature and pressure measurement, and working fluid mass flow rate measurement. The specific thermodynamic characteristics of siloxane MDM, including a low or moderate temperature change even with high turbine pressure ratios, highlights the need for accurately measuring the thermodynamic state at the turbine inlet and outlet. It was concluded that the original measurement system was not accurate enough to accurately estimate the turbine performance in the tests. Thus, an improved measurement system is now adopted, which includes improved turbine outlet state measurement and mass flow rate measurements. In addition, pressure measurement points are added to turbine stator nozzles in order to estimate the operation and performance of the stator more accurately, as well as to evaluate how the expansion is divided between the stator and rotor during the experiments. The overall objective of the updates to the measurement system is to collect accurate experimental data on the operation and losses of small-scale high expansion ratio radial turbines for ORC applications.

Figure 1a shows the fundamental derivative of gas dynamics Γ and compressibility factor Z along the isentropic expansion from turbine inlet to outlet states at the design point. At the turbine design operating point, as well as in the typical operating conditions of the turbine, both the value of Γ and Z are well below 1 at the beginning of the expansion and the values are approaching unity at the turbine outlet. This indicates that the turbine is operated in non-ideal thermodynamic conditions, and the vapor expansion is highly non-ideal especially in the turbine stator. Non-ideal phenomena like the non-monotone development of Mach number along the expansion can also be encountered. An image of the turbine used in the experimental system is shown in Figure 1b. The turbine has a supersonic stator with outlet Mach number of 2.4 and a radial turbine impeller.

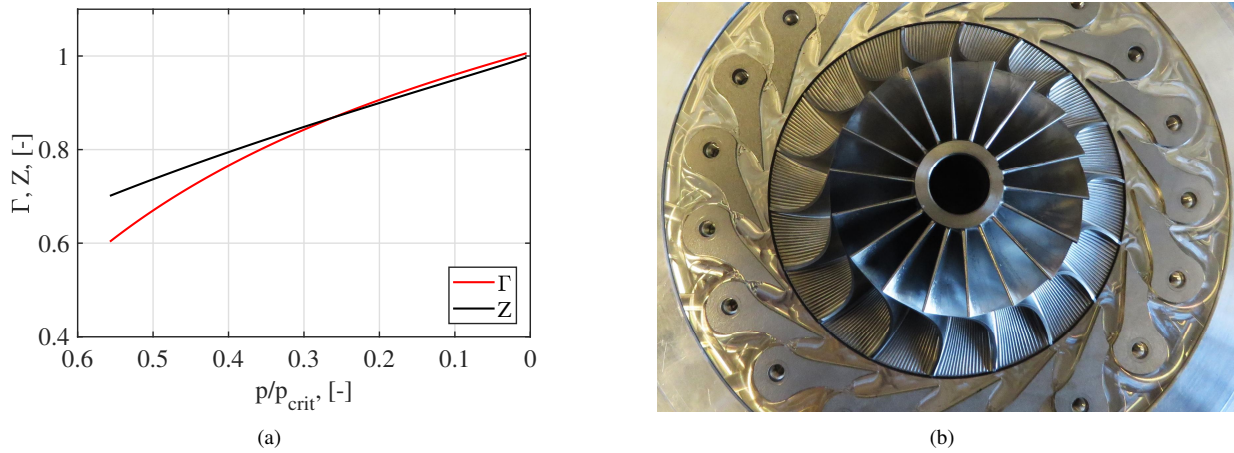


Figure 1: a) Fundamental derivative of gas dynamics (Γ) and compressibility factor (Z) under isentropic expansion from turbine design inlet conditions to turbine design outlet pressure. b) Supersonic radial turbine of the experimental setup

2 EXPERIMENTAL SETUP

2.1 Turbine measurements

The turbine experiments with the original measurement system were carried out between 2016-2019 [5]. When analysing the test results it was observed that defining the turbine isentropic efficiency from the experimental data is sensitive especially on the accuracy of the temperature measurement at the turbine outlet. During the experimental campaign with the original measurement setup, the turbine efficiency was, on average, over 70 % [5]. However, it was estimated that even a small deviation of 1-2 K in the turbine outlet temperature has a high impact (from about 3 % to almost 6 %) on the defined turbine isentropic efficiency, if compared to the estimated turbine efficiency in design conditions.

The sensitivity of turbine outlet temperature on turbine isentropic efficiency with turbine design inlet conditions and design outlet pressure is presented in Figure 2a. During the experiments, the turbine outlet temperature measurement had some fluctuations resulting in high uncertainties in the turbine efficiency estimation defined from the measured data. Especially, these fluctuations in the measured turbine outlet temperature were observed to be more significant when running the turbogenerator at relatively low speeds, whereas with turbogenerator rotational speeds approaching the design speed, the measured turbine outlet temperature is more in line with the predictions of thermodynamic cycle models with less fluctuations during the operation [5]. An example of measured temperature drops over the turbine as a function of turbine pressure ratio and the isentropic temperature drop for the respective conditions are presented

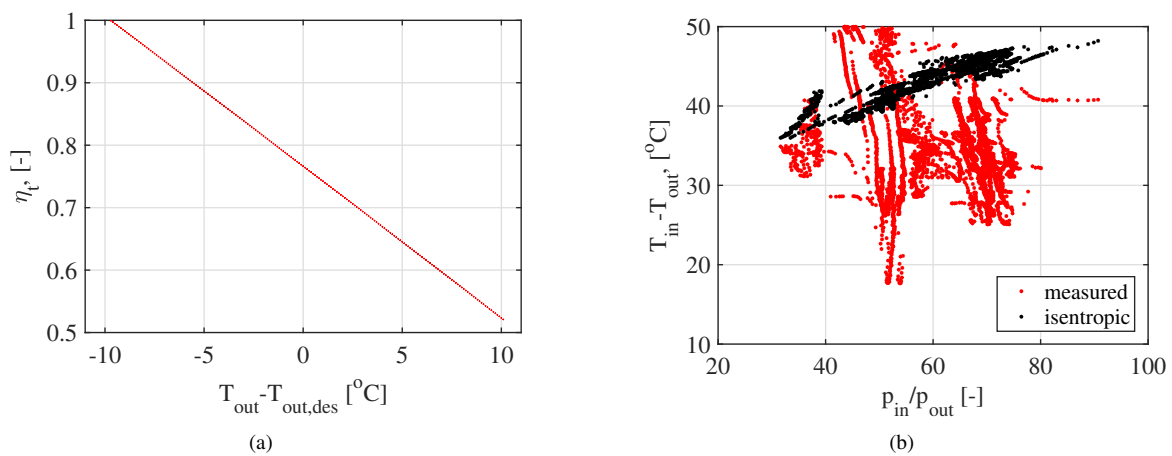


Figure 2: (a) Sensitivity of turbine outlet temperature on turbine isentropic efficiency with turbine design inlet conditions and design outlet pressure. (b) Measured temperature drop over the turbine and isentropic enthalpy change defined from measured turbine inlet conditions and outlet pressure

Table 1: Measurement equipment

	Manufacturer	Type	Accuracy
Pressure	Gems	TR2200, [0-1,0-16 bar(abs)]	$\pm 0.25\%$ full scale
Temperature	Aplisens	CT-GN1	± 0.35 K (at 100 °C temperature)
Flow rate (liquid)	Kytola Instruments	oval gear SRP-40-H	$\pm 0.5\%$
Flow rate (vapor)	McCrometer	V-cone VB0CAE01N	$\pm 0.5\%$

in Figure 2b. The data shown in Figure 2b are collected from measurement points of several test runs with the original measurement system containing data with different turbogenerator rotational speeds ranging from about 12 000 rpm to 30 000 rpm. The enthalpy drop over the turbine was based on the turbine inlet and outlet temperature measurements and the corresponding isentropic temperature drop was defined from the turbine inlet measurements and from turbine outlet pressure measurement. It can be observed that there is notable scattering of data especially at turbine pressure ratios between 40 to 60 and there are several measurement points where the measured temperature drop is even higher than the isentropic temperature drop at the respective conditions. On the other hand, with the higher pressure ratios between 60 to 80 there are less variations in the data and the measured temperature drops are at the expected range on average. It should be noted that in the majority of the data points with turbine pressure ratios between 60 to 80, the turbogenerator rotational speed has been relatively close to the turbine design rotational speed (from 24 000 rpm to 31 000 rpm), whereas the conditions with lower turbine pressure ratios are mainly representing operating conditions with turbogenerator rotational speeds below 23 000 rpm. The variations in the measured turbine outlet temperatures and in data presented in Figure 2b might be originating from both measurement accuracy and internal flows that might disturb the turbine outlet temperature measurement. One example of such internal flow could be a leakage of working fluid through the turbogenerator labyrinth seals to the turbine outlet, cooling down the turbine outlet temperature at some operating conditions. A more detailed analysis on the turbine performance under different operating conditions defined with the original measurement system and discussions on the potential sources of uncertainty in the turbine measurements are given in [5].

The turbine measurement system has been updated to allow more accurate turbine measurements. The original measurement system is shown in Figure 3a and the updated measurement system is shown in Figure 3b. The information on the measurement equipment and the sensor types are given in Table 1. In the updated system, a V-cone sensor is added after the evaporator to measure the flow rate of the vapor working fluid entering the turbine. Besides increasing the reliability of the flow rate measurement, this second flow meter allows to detect the possible accumulation of working fluid in the evaporator. An oval gear meter is used for measuring the flow of liquid working fluid entering the evaporator. Two additional temperature sensors have been installed at turbine outlet to reduce the uncertainties in the turbine outlet condition measurements, since in the old setup the turbine outlet temperature was measured by using only one sensor. The positioning of the three temperature sensors at the turbine outlet duct is presented in Figure 4. The increased number and the placement of turbine outlet temperature sensors will help detecting the possible malfunctions in individual sensors as well as in detecting the possibility of uneven temperature distributions of the turbine discharge flow that can effect on the efficiency definition from the measurements. In addition, a second pressure probe was added at the turbine outlet to increase the reliability of the turbine outlet pressure measurement.

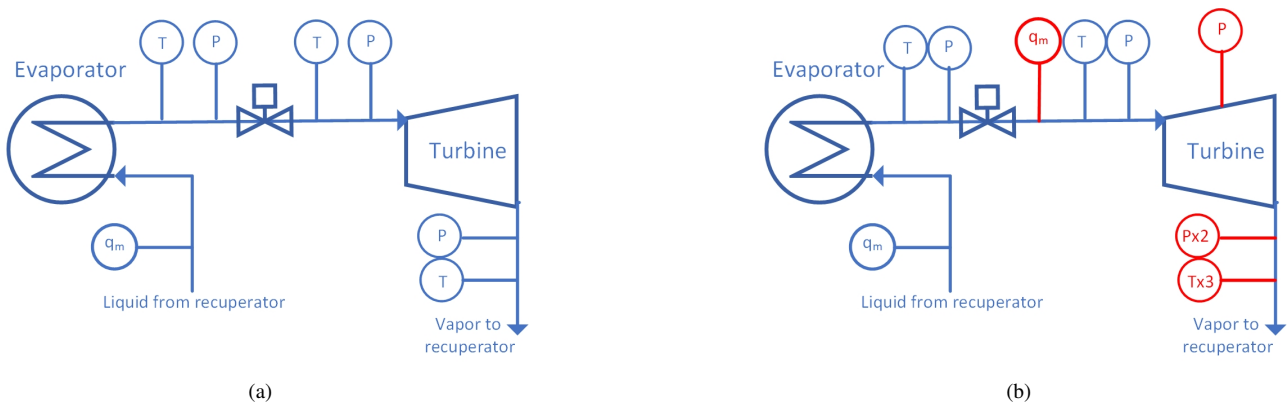


Figure 3: (a) Original turbine related measurements and (b) updated turbine measurements. P = pressure measurement, T = Temperature measurement, q_m = flow measurement



Figure 4: Positioning of the temperature sensors at the turbine outlet duct

2.2 Pressure measurements inside the turbine stator

During a single experimental run, the operating conditions of the turbine experience significant variations. Pressure measurement points are added inside the turbine stator in order to monitor the expansion along the blade passages at varying operating point. Figure 1b shows the top view of the radial turbine of the experimental setup. The 19 blades of the stator ring delimit converging-diverging planar nozzles, with throat width 1.3 mm and blade height 2 mm. The stator has internal diameter 145 mm and external diameter 230 mm. Access to the flow is possible from the stator back plate visible in Figure 1b. There, static-pressure wall tapings are machined at the positions highlighted in Figure 5, and pressure is measured along the blade passages. This paragraph describes the measurement system and discusses the rationale behind the choice of measurement locations.

The most relevant constraint to implementing a measurement system inside the stator is represented by the small size of the stator ring. Indeed, conventional machining processes limit the minimum obtainable diameter of pressure taps to 0.5 mm, which compared to the characteristic lengths of the blade passages reads $\sim 1/3$ of the throat width and $1/4$ of the blade height. First, the spatial pressure gradient experienced by the expanding flow at the surface of pressure taps can be relevant due to the large relative size of wall tapings with respect to the blade passage. Second, cavity-like flow patterns are expected to occur past the exposed edges of pressure taps due to

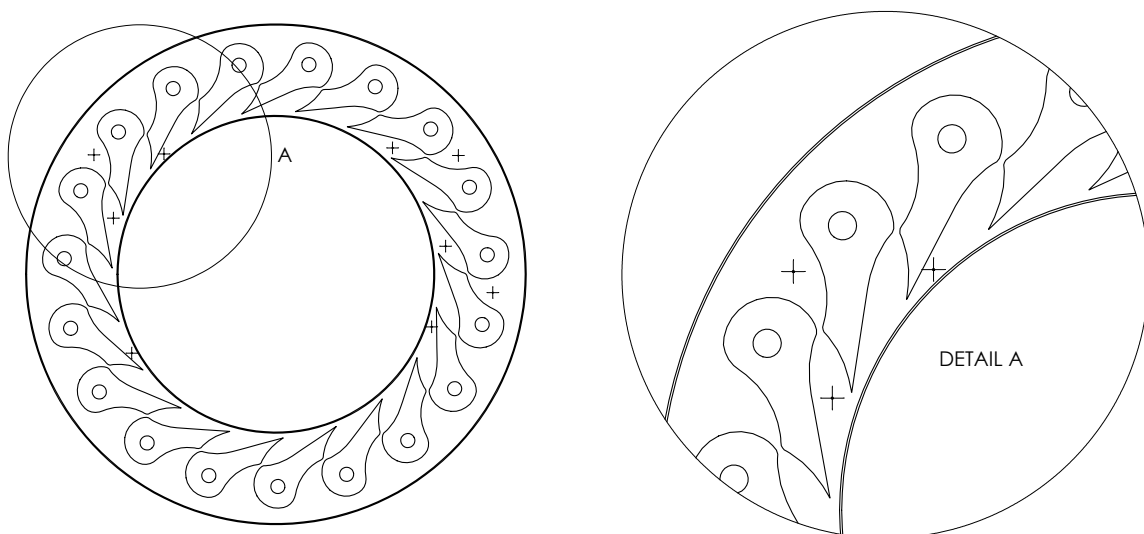


Figure 5: Drawing of the stator ring (to scale), equipped with pressure taps (center markings). Pressure measurement points are located in the convergent and in the divergent, both upstream and downstream of the trailing-edge shocks

interaction with the main flow. Though the intrusiveness of the measurement system cannot be eliminated, mitigation of its effects can be achieved by carefully selecting the position of measurement points.

Results of detailed numerical analyses of the stator flow-field are examined in order to identify the regions characterized by low spatial pressure gradient. Reference results are those documented in Ref. [4], which include two-dimensional Navier-Stokes simulation of design and off-design operation of the stator. Further 2D Navier-Stokes simulations are performed in this study (Figure 6) using ANSYS Fluent v19.4, RefProp v7.0 database, and $k-\omega$ SST turbulence model. Figures 6a and 6b show the pressure distribution inside a stator channel at the design operating point (total pressure 7.9 bar, total temperature 538.15 K, and stator outlet pressure 0.4 bar). Figure 6a reports pressure isolines in the nozzle, while Figure 6b shows the pressure (blue) and pressure gradient (red) profiles along the nozzle centreline, i.e. along yellow line in Figure 6a. In Figure 6b, the origin of the x axis is placed at the throat section. Results show that the expansion from inlet to outlet pressure levels occurs mostly in a 10 mm-long region close to the nozzle throat, where the pressure gradient reaches ~ 3 bar/mm. Pressure experiences another sharp variation across the trailing-edge shock wave. Elsewhere, the pressure gradient is significantly smaller. Three radial locations are selected, one in the convergent, one in the divergent upstream of the trailing-edge shocks, and one at stator outlet past the trailing-edge shocks, see Figure 5. At the selected locations, pressure gradient is < 20 mbar/mm, and the pressure variation across the surface of pressure taps is within the accuracy of pressure transducers.

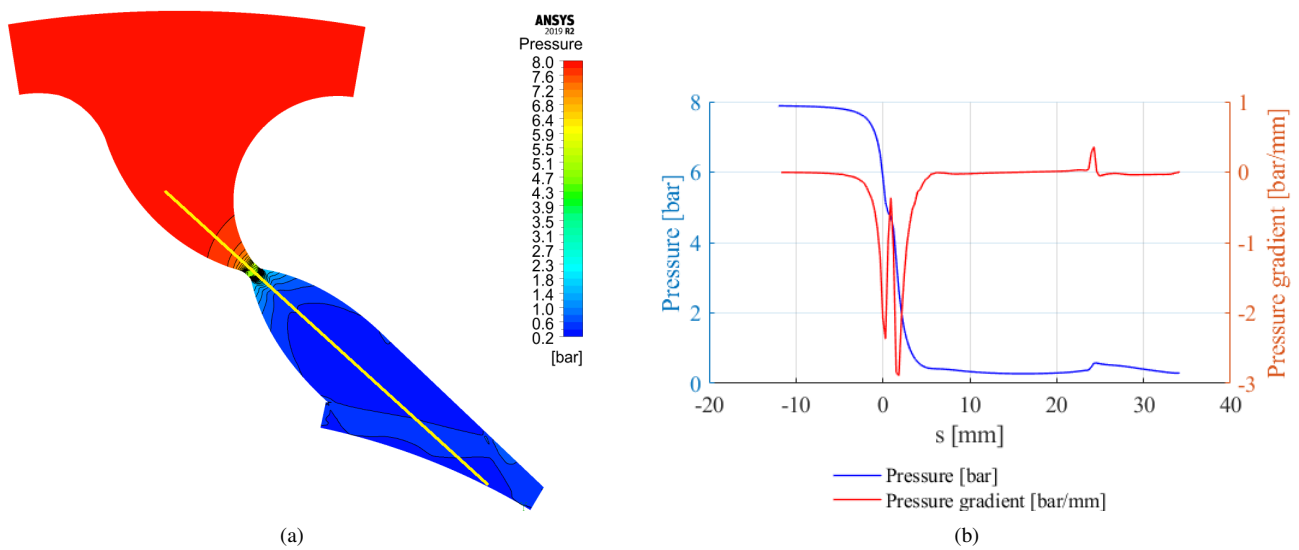


Figure 6: (a) Pressure distribution within the stator channel in design conditions (b) Pressure and pressure gradient profiles along the yellow line of Figure 6a

A quantitative analysis of cavity flows past the edges of wall tapplings is not performed in this study. However, their occurrence is considered and its impact on the final pressure readings is analyzed. Given the low diameter/depth ratio of wall tapplings, an open-cavity flow configuration is expected to occur, see e.g. Ref. [3], with flow separation at the upstream edge of the tapping, recirculation inside the cavity, and reattachment at the downstream edge. The incoming flow experiences a slight expansion at the upstream edge of the tapping, followed by a recompression at the downstream one. In the supersonic regions of the flow, these phenomena are accompanied by expansion and compression waves, which will propagate and perturb the main flow. Though the final pressure readings are not expected to depart significantly from the target pressure levels, it is unclear to which extent these perturbations will affect the main flow during the experiments. For this reason, all tapplings are located relatively far from the blade profiles, and pressures upstream and downstream of trailing-edge shocks are measured in separate blade passages. In order to evaluate flow uniformity around the stator ring, and to check the validity of pressure readings at each radial location, three sets of measurement points are used at different angular positions (cf. Figure 5).

Industrial transducers of the same model adopted for pressure measurements at turbine inlet and outlet are employed, see the first line of Table 1. Transducers with full scale 16 bar(abs) and 1 bar(abs) are used, respectively, in the subsonic and supersonic regions. The accuracy of transducers is within $\pm 0.25\%$ of full scale, while their response time is ~ 0.5 ms. Transducers are connected to the wall tapplings through a pressure line. A linear analysis of the resulting pressure line-cavity system is carried out according to the formulation presented in Ref. [6], which yields an estimated maximum response time of about 10 ms.

Combined with pressure and temperature measurements at turbine inlet and outlet, pressure measurements inside the stator allow to quantify the contribution of stator and rotor to the overall turbine expansion, and to estimate trailing-edge shock losses. Moreover, since the expansion in the stator occurs in the non-ideal flow regime, a dependence of the expansion profile on the total conditions is expected to be observed, though perhaps not directly inferrable from measurements due to the relatively large measurement uncertainties.

3 CONCLUSIONS AND FUTURE WORKS

The design of an updated measurement system for the LUT 10 KW micro ORC test-rig is presented. Further instrumentation is adopted to improve the performance analysis of the cycle and its components, especially of the radial turbine. A better characterization of turbine efficiency is achieved through an increased sensor redundancy, namely with an additional flow meter ahead of the turbine and duplication of temperature and pressure probes at turbine outlet. Pressure measurement points are also added inside the turbine stator ring to characterize the supersonic expansion along the stator blade passages, to estimate trailing-edge shock losses, and to assess how the expansion is divided between the stator and rotor during the experiments.

The updated measurement system is currently being commissioned, and the first experimental campaign will be carried out in Autumn 2020. From the acquired data and the use of state-of-the-art thermodynamic models, detailed performance maps of the operation and losses of the system will be redacted, and the influence of flow non-ideality on the performance parameters will be investigated. Experimental data will also be used to validate the numerical models of the turbine flow-field in design and off-design conditions.

REFERENCES

References

- [1] P. Colonna, E. Casati, C. Trapp, T. Mathijssen, J. Larjola, T. Turunen-Saaresti, and A. Uusitalo. Organic rankine cycle power systems: from the concept to current technology, applications, and an outlook to the future. *Journal of Engineering for Gas Turbines and Power*, 137(10), 2015.
- [2] J. R. Seume, M. Peters, and H. Kunte. Design and test of a 10kw orc supersonic turbine generator. *Journal of Physics: Conference Series*, 821(1):012023, 2017.
- [3] R. L. Stallings and F. J. Wilcox. Experimental cavity pressure distributions at supersonic speeds. Technical Report Technical Paper 2683, NASA, 1987.
- [4] A. Uusitalo. *Working fluid selection and design of small-scale waste heat recovery systems based on Organic Rankine Cycles*. PhD thesis, Lappeenranta-Lahti University of Technology, 2014.
- [5] A. Uusitalo, T. Turunen-Saaresti, J. Honkatukia, and R. Dhanasegaran. Experimental study of small scale and high expansion ratio orc for recovering high temperature waste heat. *Energy*, 208, 2020.
- [6] VKI-LS-2001-04. *Measurement techniques in fluid dynamics*. VKI, 2009.
- [7] P. A. Weiss, T. Popp, J. Müller, J. Hauer, D. Brüggemann, and M. Preissinger. Experimental characterization and comparison of an axial and a cantilever micro-turbine for small-scale organic rankine cycle. *Applied Thermal Engineering*, 140:235–244, 2018.

NOMENCLATURE

Roman symbols

p	Pressure
q_m	Flow rate
T	Temperature

Greek symbols

Γ	Fundamental derivative of gas dynamics
Z	Compressibility factor

Sub- and super-indices

crit	Critical
des	Design point
out	Outlet